

## Europium(III) DOTA-tetraamide Complexes as Redox-Active MRI Sensors

S. James Ratnakar,<sup>†</sup> Subha Viswanathan,<sup>†</sup> Zoltan Kovacs,<sup>†,‡</sup> Ashish K. Jindal,<sup>†</sup> Kayla N. Green,<sup>†</sup> and A. Dean Sherry<sup>\*,†,‡</sup>

<sup>†</sup>Advanced Imaging Research Center, University of Texas Southwestern Medical Center, 5323 Harry Hines Boulevard, Dallas, Texas 75390, United States

<sup>‡</sup>Department of Chemistry, University of Texas, Dallas, 800 West Campbell Road, Richardson, Texas 75080, United States

### S Supporting Information

**ABSTRACT:** PARACEST redox sensors containing the NAD<sup>+</sup>/NADH mimic *N*-methylquinolinium moiety as a redox-active functional group have been designed and synthesized. The Eu<sup>3+</sup> complex with two quinolinium moieties was nearly completely CEST-silent in the oxidized form but was “turned on” upon reduction with β-NADH. The CEST effect of the Eu<sup>3+</sup> complex containing only one quinolinium group was much less redox-responsive but showed an unexpected sensitivity to pH in the physiologically relevant pH range.

Proper regulation of the cellular redox state is critical to many fundamental biochemical processes. Localized changes in the redox potential have been shown to play an important role in signal transduction influencing a wide variety of cellular functions.<sup>1</sup> Despite its biological significance, currently there is no convenient noninvasive method for mapping the ambient redox potential in living tissues. Magnetic resonance imaging (MRI) is a powerful noninvasive diagnostic tool, and promising results have been achieved in the development of various redox-sensitive Gd<sup>3+</sup>- and Mn<sup>2+/3+</sup>-based (*T*<sub>1</sub>-shortening) contrast agents.<sup>2–4</sup> Over the past decade, chemical exchange saturation transfer (CEST) agents have evolved as a viable alternative to traditional *T*<sub>1</sub> agents, especially in the adaptation of MRI to molecular imaging.<sup>5,6</sup> 1,4,7,10-Tetraazacyclododecane-1,4,7,10-tetraacetic acid (DOTA)-tetraamide complexes of paramagnetic hyperfine shifting Ln<sup>3+</sup> ions, in particular Eu<sup>3+</sup>, induce large paramagnetic shifts of the metal-bound water protons and have sufficiently low water exchange rates to satisfy the slow-to-intermediate exchange condition ( $k_{ex} \leq \Delta\omega$ ) for CEST.<sup>6,7</sup>

It has been demonstrated that comparatively small changes in the structure of the coordinating amide side arms of Eu<sup>3+</sup> DOTA-tetraamide complexes can generate large changes in the frequency and/or magnitude of the CEST effect originating from the metal-bound water molecule.<sup>8–10</sup> Our approach for developing redox-sensitive MRI agents relies on this sensitivity of the CEST signal on the water exchange rate.<sup>11</sup> When one or more redox-active groups are attached to the coordinating pendant arms of a Eu<sup>3+</sup> chelate, the redox status of the reporter group should have a detectable influence on the CEST signal. We have shown previously that the oxidized and reduced forms of a Eu<sup>3+</sup> DOTA-tetraamide complex containing a *p*-nitro-

phenylamide functionality could be discriminated by CEST spectroscopy and MRI.<sup>8</sup> However, this complex cannot be used as an *in vivo* redox sensor because the redox potential of this system is outside the biologically relevant range. Our design for a potentially biocompatible redox-active CEST agent is based on the reversible redox reactivity of the nicotinamide moiety in the nicotinamide adenine dinucleotide (NAD<sup>+</sup>/NADH) coenzyme system.<sup>12,13</sup> Several nicotinamide, quinoline, and acridine derivatives that are capable of mimicking the function of NAD<sup>+</sup>/NADH have been reported. While the pyridinium/1,4-dihydropyridine redox systems are the closest analogues to NAD<sup>+</sup>/NADH, these compounds are extremely susceptible to degradation in aqueous solution. Quinoline derivatives are significantly more stable and still display reasonable reactivity in biomimetic reductions.<sup>14</sup> Our hypothesis was that reduction of the quinolinium moiety to the dihydroquinoline derivative would induce a sufficient change in the coordination environment around the lanthanide ion to modulate the water exchange lifetime of the Eu<sup>3+</sup>-bound water molecule. Using these principles, we have designed and synthesized two Eu<sup>3+</sup> DOTA-tetraamide complexes, Eu<sup>3+</sup>-(1) and Eu<sup>3+</sup>-(2) (Figure 1),

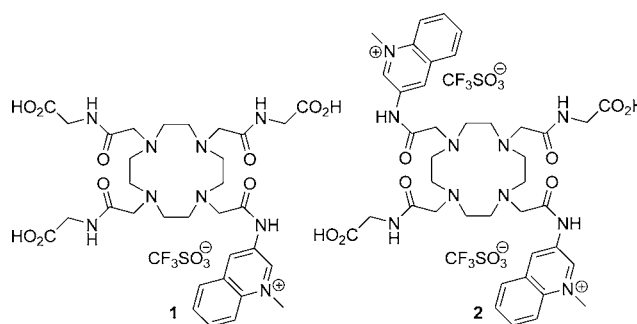


**Figure 1.** Quinolinium DOTA-tetraamide derivatives examined in this work.

containing one and two quinolinium groups attached to the pendant arms of the DOTA-tetraamide moiety, respectively. The ligands were synthesized by alkylating the *tert*-butyl esters of DO3A-(gly)<sub>3</sub> or DO2A-(gly)<sub>2</sub> with 3-bromoacetamidoquinoline followed by quaternization of the quinoline N atom with

**Received:** December 23, 2011

**Published:** March 15, 2012

methyl triflate [synthetic details are given in Schemes S1–S3 in the Supporting Information (SI)].

The  $^1\text{H}$  NMR spectra of  $\text{Eu}^{3+}$ -(1) and  $\text{Eu}^{3+}$ -(2) in  $\text{D}_2\text{O}$  showed a resonance at 25 ppm characteristic of four H4 macrocyclic protons in  $\text{Eu}^{3+}$  complexes of this type that exist in solution in a square-antiprism (SAP) coordination geometry as the major isomer (Figure S1 in the SI).<sup>7,11</sup> Nonenzymatic reduction of the quinolinium moiety of  $\text{Eu}^{3+}$ -(1) occurred rapidly after addition of 1 equiv of  $\beta$ -NADH (pH 7), resulting in the formation of the reduced form of the complex (Figure S2).<sup>15</sup> Other reducing agents such as  $\text{Na}_2\text{S}_2\text{O}_4$  and  $\text{NaBH}_4$  also reduced the quinolinium moiety in  $\text{Eu}^{3+}$ -(1), resulting in a similar change in CEST.<sup>16,17</sup> In analogy to NADH model compounds, we suggest that the quinolinium ring on the pendant arm of the DOTA scaffold is reduced predominantly to the 1,4-dihydroquinoline derivative, even though we could not establish the structure of the reduced products unequivocally.<sup>15</sup> Interestingly, the  $\text{Eu}^{3+}$  complex in which the quinoline N atom is not methylated does not undergo reduction by  $\beta$ -NADH and shows no change in CEST (Figure S3). This observation indicates that the quaternary nitrogen of the quinolinium ring is essential for reduction to occur. The CEST signal arising from exchange of the  $\text{Eu}^{3+}$ -bound water molecule in  $\text{Eu}^{3+}$ -(1) increased in intensity somewhat, became sharper (indicative of slower exchange), and shifted from 48 to 53 ppm upon reduction. The bound-water lifetimes ( $\tau_M$ ) for the oxidized and reduced forms estimated by fitting the experimental CEST spectra to the Bloch equations modified for exchange were 78 and 130  $\mu\text{s}$ , respectively. In comparison, the  $\tau_M$  of the parent  $\text{Eu}[\text{DOTA}-(\text{gly})_4]^-$  agent is  $\sim 160$   $\mu\text{s}$ . One can thus conclude that substitution of aminoquinoline for a single glycine on the side arm of  $\text{DOTA}-(\text{gly})_4$  results in about a 2-fold increase in the water exchange rate in the resulting  $\text{Eu}^{3+}$  complexes. It is worth noting that the lower water exchange rate of the reduced form is somewhat counterintuitive, as one might have anticipated the oxidized species to have slower water exchange because of the presence of the more electron-withdrawing positively charged methylquinolinium moiety.<sup>11</sup>

The reaction of  $\text{Eu}^{3+}$ -(2) with 2 equiv of  $\beta$ -NADH in water at pH 7 also gave a reduced complex. Interestingly, the CEST signal increased in intensity much more dramatically in  $\text{Eu}^{3+}$ -(2) (from 2 to 15%) upon reduction than in  $\text{Eu}^{3+}$ -(1). The CEST peak of  $\text{Eu}^{3+}$ -(2) also displayed a larger 7 ppm shift (from 43 to 50 ppm; see Figure 2). As expected, the water exchange lifetime of the reduced form of  $\text{Eu}^{3+}$ -(2) (90  $\mu\text{s}$ ) was

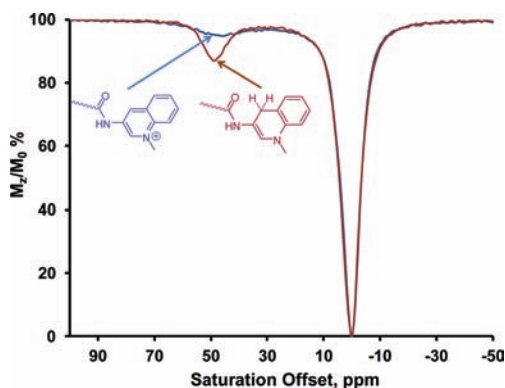


**Figure 2.** CEST spectra of the oxidized (blue) and reduced (red) forms of  $\text{Eu}^{3+}$ -(2) (20 mM) collected at 9.4 T, pH 7, 298 K, and  $B_1 = 10$   $\mu\text{T}$  with a presaturation time of 5 s.

found to be significantly shorter than that in reduced  $\text{Eu}^{3+}$ -(1). The  $\tau_M$  for the oxidized form could not be determined because of the small magnitude of the CEST effect even at high  $B_1$  power, but the broad width of the CEST peak indicates that water exchange was faster in the oxidized form of  $\text{Eu}^{3+}$ -(2) than in  $\text{Eu}^{3+}$ -(1).

The redox properties of these complexes were examined by cyclic voltammetry. Two well-separated redox peaks corresponding to the two-electron reduction of the quinolinium ring to the dihydroquinoline were detected for  $\text{Eu}^{3+}$ -(1). However, the redox couple appeared to be quasi-reversible since the reduced form was not completely oxidized when an anodic current was applied. It is likely that the fully reduced dihydroquinoline derivative or its precursor species is susceptible to degradation in aqueous solutions and that the incomplete oxidation during the anodic scan was due to the partial decomposition of the reduced derivative.  $\text{Eu}^{3+}$ -(2) displayed a similar cyclic voltammogram under identical experimental conditions (Figure S5). In addition, this behavior was also seen in the cyclic voltammogram of the free ligand (2) indicating that the redox reaction occurs at the quinolinium moiety and that the  $\text{Eu}^{3+}$  ion is not involved.<sup>18</sup>

While CEST from the exchanging water molecule is generally independent of pH,<sup>6</sup> the CEST signal of  $\text{Eu}^{3+}$ -(1) showed a surprisingly strong pH sensitivity (Figure 3). The bound-water

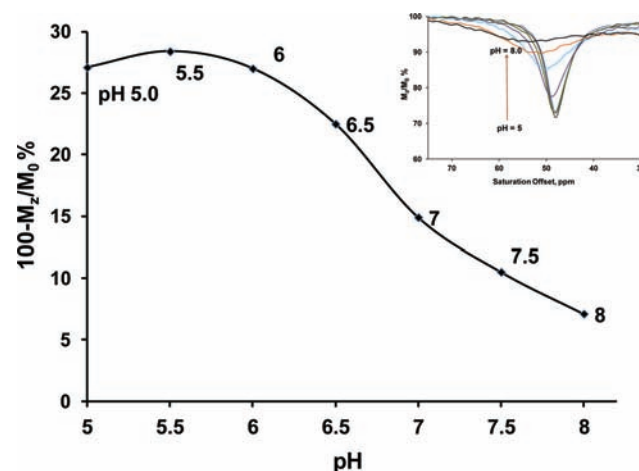


**Figure 3.** pH dependence of the metal-bound water CEST signal of  $\text{Eu}^{3+}$ -(1) (20 mM) at 9.4 T, 298 K, and  $B_1 = 10$   $\mu\text{T}$  with an irradiation time of 5 s. The inset shows CEST spectra collected at each pH.

CEST peak at 48 ppm gradually broadened and decreased in intensity when the pH was increased from 5 to 8 (Figure 3 inset). Although the exact mechanism of this pH responsiveness is yet unknown, the broadening of the CEST peak at higher pH suggests that this effect may be due to base-catalyzed deprotonation of the amide NH attached to the strongly electron-withdrawing quaternized quinoline ring, which in turn increases the water exchange rate. This assumption is supported by the fact that the CEST signal of the nonmethylated form of  $\text{Eu}^{3+}$ -(1) showed only a negligible pH dependence over the same pH range. The pH-dependent CEST is an interesting feature of  $\text{Eu}^{3+}$ -(1) and may provide ideas for the design of future pH-responsive agents. In comparison,  $\text{Eu}^{3+}$ -(1) after reduction with  $\beta$ -NADH did not show a significant pH-responsive behavior.

To demonstrate that the oxidized and reduced forms can be distinguished by MRI, CEST imaging of a phantom containing the oxidized and reduced species of  $\text{Eu}^{3+}$ -**(2)** (the latter generated by adding 2 equiv of  $\beta$ -NADH) was performed. The images were collected at 9.4 T using a modified fast spin echo sequence at 298 K. A 10  $\mu\text{T}$  saturation pulse was applied for 3 s prior to collection of the image. The CEST images were generated by subtracting the saturation-on image from the saturation-off image. In agreement with the CEST spectra, the tube containing the reduced form showed a higher image intensity in the difference images in comparison with the oxidized form (Figure 4).

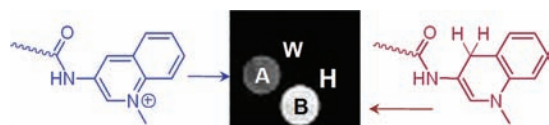


**Figure 4.** PARACEST images acquired for a phantom containing four tubes: (A)  $\text{Eu}^{3+}$ -**(2)** (20 mM) in HEPES buffer (pH 7, 0.25M); (B)  $\text{Eu}^{3+}$ -**(2)** (20 mM) plus 2 equiv of  $\beta$ -NADH in HEPES buffer (pH 7, 0.25M); (W) water; (H) HEPES buffer at pH 7.

In conclusion, we have reported the first activatable PARACEST redox sensor. We have incorporated an *N*-methylquinolinium moiety (an  $\text{NAD}^+/\text{NADH}$  analogue) as a redox-active functional group onto the pendant arm of the DOTA-tetraamide scaffold. The complex  $\text{Eu}^{3+}$ -**(2)** with two quinolinium moieties was nearly completely CEST-silent while in the oxidized form but was “turned on” upon reduction with  $\beta$ -NADH. This makes  $\text{Eu}^{3+}$ -**(2)** a good candidate for further development as a responsive redox sensor. The CEST signal of the  $\text{Eu}^{3+}$  complex containing only one quinolinium group was much less redox-responsive but showed an unexpected sensitivity to pH over the physiologically relevant pH range.

## ■ ASSOCIATED CONTENT

### 📄 Supporting Information

Synthetic procedure, experimental details,  $^1\text{H}$  NMR spectroscopy, CEST spectra as a function of applied  $B_1$ , CEST fitting data, and electrochemical data. This material is available free of charge via the Internet at <http://pubs.acs.org>.

## ■ AUTHOR INFORMATION

### Corresponding Author

dean.sherry@utsouthwestern.edu

### Notes

The authors declare no competing financial interest.

## ■ ACKNOWLEDGMENTS

The authors acknowledge partial financial support for this work from the National Institutes of Health (CA-115531, CA-126608, RR-02584, and EB-00482) and the Robert A. Welch Foundation (AT-584).

## ■ REFERENCES

- (1) Stryer, L. *Biochemistry*; 3rd ed.; Freeman: New York, 1988.
- (2) Tu, C.; Nagao, R.; Louie, A. Y. *Angew. Chem., Int. Ed.* **2009**, *48*, 6547–6551.
- (3) Raghunand, N.; Jagadish, B.; Trouard, T. P.; Galons, J.-P.; Gillies, R. J.; Mash, E. A. *Magn. Reson. Med.* **2006**, *55*, 1272–1280.
- (4) Aime, S.; Botta, M.; Gianolio, E.; Terreno, E. *Angew. Chem., Int. Ed.* **2000**, *39*, 747–750.

- (5) Ward, K. M.; Aletras, A. H.; Balaban, R. S. *J. Magn. Reson.* **2000**, *143*, 79–87.
- (6) Viswanathan, S.; Kovacs, Z.; Green, K. N.; Ratnakar, S. J.; Sherry, A. D. *Chem. Rev.* **2010**, *110*, 2960–3018.
- (7) Zhang, S.; Winter, P.; Wu, K.; Sherry, A. D. *J. Am. Chem. Soc.* **2001**, *123*, 1517–1518.
- (8) Ratnakar, S. J.; Woods, M.; Lubag, A. J. M.; Kovacs, Z.; Sherry, A. D. *J. Am. Chem. Soc.* **2008**, *130*, 6–7.
- (9) Viswanathan, S.; Ratnakar, S. J.; Green, K. N.; Kovacs, Z.; De Leon-Rodriguez, L. M.; Sherry, A. D. *Angew. Chem., Int. Ed.* **2009**, *48*, 9330–9333.
- (10) Mani, T.; Tircso, G.; Togao, O.; Zhao, P.; Soesbe, T. C.; Takahashi, M.; Sherry, A. D. *Contrast Media Mol. Imaging* **2009**, *4*, 183–191.
- (11) Woessner, D. E.; Zhang, S.; Merritt, M. E.; Sherry, A. D. *Magn. Reson. Med.* **2005**, *53*, 790–799.
- (12) Gomez, E.; Miguel, M.; Jimenez, O.; De la Rosa, G.; Lavilla, R. *Tetrahedron Lett.* **2005**, *46*, 3513–3516.
- (13) Ostovic, D.; Lee, I. S. H.; Roberts, R. M. G.; Kreevoy, M. M. *J. Org. Chem.* **1985**, *50*, 4206–4211.
- (14) Mikata, Y.; Mizukami, K.; Hayashi, K.; Matsumoto, S.; Yano, S.; Yamazaki, N.; Ohno, A. *J. Org. Chem.* **2001**, *66*, 1590–1599.
- (15) Creighton, D. J.; Hajdu, J.; Mooser, G.; Sigman, D. S. *J. Am. Chem. Soc.* **1973**, *95*, 6855–6857.
- (16) Wong, Y. S.; Marazano, C.; Gnecco, D.; Das, B. C. *Tetrahedron Lett.* **1994**, *35*, 707–710.
- (17) Bunting, J. W.; Meathrel, W. G. *Tetrahedron Lett.* **1971**, 133–136.
- (18) Blaedel, W. J.; Haas, R. G. *Anal. Chem.* **1970**, *42*, 918–927.